QUANTITATIVE STUDY OF NANOSCALE CONTACT AND PRE-CONTACT MECHANICS USING FORCE MODULATION

S.A. SYED ASIF*, K.J. WAHL** AND R.J. COLTON**
*Dept. of Materials Science and Engineering, University of Florida, Gainesville, FL 32611
**Code 6170, Chemistry Division, Naval Research Laboratory, Washington, DC 20375-5342

ABSTRACT

For submicron-scale mechanical property measurements, depth sensing nanoindentation techniques are very successful and gaining much attention. However, for ultra-small volumes of materials below a length scale of 10 nm, measuring the quantitative mechanical properties of materials is still a problem. The atomic force microscope (AFM) has very good surface sensitivity and has been shown to measure nanomechanical properties. However cantilever instability, conventional force detection and displacement sensing make contact area measurement difficult, hence the measured mechanical properties are usually only qualitative. In this article, we show that combining force modulation with depth sensing nanoindentation allows measurement of the mechanical properties of materials on the nanometer scale. With this technique we have studied the role of oxide layers on the mechanical response of Si surfaces. We also present a novel quantitative stiffness imaging technique, which can be used to directly map the mechanical properties of materials with submicron lateral resolution.

INTRODUCTION

The quantitative study of the mechanical properties of materials at the nanoscale has been receiving much attention in recent years. These studies have been motivated by the development of new nanostructured materials and continued miniaturization of engineering and electronic components, thin film technology and surface coatings. For submicron-scale mechanical property measurement, depth sensing nanoindentation techniques are very successful and gaining attention [1]. However, due to poor surface sensitivity, difficulty in characterizing the tip shape, unknown thermal drift and floor noise, measuring the quantitative mechanical properties at depths less than 10 nm is extremely difficult. To measure the response of monolayers or nanometer thick surface layers, the measuring instrument must have good surface sensitivity. To avoid this problem, we have recently implemented a force modulation technique coupled with nanoindentation using a three-plate capacitive load-displacement transducer [2]. The stiffness sensitivity of the technique is 0.1 N/m, which is sufficient to detect long-range surface forces and locate the surface of compliant materials.

In this article we report the influence of surface oxides on the nanomechanical response of Si surfaces using a combined depth sensing and force modulation technique. We have measured the mechanical properties of the surface oxide layer quantitatively for contact depths less than 5 nm. We show that the oxide layer on the Si surface is more compliant than the Si substrate and the mechanical response is dependent on thickness of the oxide layer. We also show that the force modulation technique can be used to map quantitatively the mechanical response over an area.

Report Documentation Page

Form Approved
OMB No. 0704-0188

Public reporting burden for the collection of information is estimated to average 1 hour per response, including the time for reviewing instructions, searching existing data sources, gathering and maintaining the data needed, and completing and reviewing the collection of information. Send comments regarding this burden estimate or any other aspect of this collection of information, including suggestions for reducing this burden, to Washington Headquarters Services, Directorate for Information Operations and Reports, 1215 Jefferson Davis Highway, Suite 1204, Arlington VA 22202-4302. Respondents should be aware that notwithstanding any other provision of law, no person shall be subject to a penalty for failing to comply with a collection of information if it does not display a currently valid OMB control number.

1. REPORT DATE **1999**	2. REPORT TYPE	3. DATES COVERED **00-00-1999 to 00-00-1999**

4. TITLE AND SUBTITLE **Quantitative Study of Nanoscale contact and Pre-Contact Mechanics Using Force Modulation**	5a. CONTRACT NUMBER
	5b. GRANT NUMBER
	5c. PROGRAM ELEMENT NUMBER
6. AUTHOR(S)	5d. PROJECT NUMBER
	5e. TASK NUMBER
	5f. WORK UNIT NUMBER

7. PERFORMING ORGANIZATION NAME(S) AND ADDRESS(ES) **Naval Research Laboratory,Code 6170,4555 Overlook Avenue, SW,Washington,DC,20375**	8. PERFORMING ORGANIZATION REPORT NUMBER

9. SPONSORING/MONITORING AGENCY NAME(S) AND ADDRESS(ES)	10. SPONSOR/MONITOR'S ACRONYM(S)
	11. SPONSOR/MONITOR'S REPORT NUMBER(S)

12. DISTRIBUTION/AVAILABILITY STATEMENT
Approved for public release; distribution unlimited

13. SUPPLEMENTARY NOTES
The original document contains color images.

14. ABSTRACT

15. SUBJECT TERMS

16. SECURITY CLASSIFICATION OF:			17. LIMITATION OF ABSTRACT	18. NUMBER OF PAGES	19a. NAME OF RESPONSIBLE PERSON
a. REPORT **unclassified**	b. ABSTRACT **unclassified**	c. THIS PAGE **unclassified**		**6**	

Standard Form 298 (Rev. 8-98)
Prescribed by ANSI Std Z39-18

EXPERIMENTAL

The material used for this study was a Si single crystal wafer with the (100) plane normal to the test surface. Two types of Si surfaces were prepared: hydrophilic and hydrophobic. Hydrophilic surfaces were prepared using a piranha etch (70% H_2SO_4 +30% H_2O_2). This etching procedure leaves the surface with a 5 nm thick oxide layer, measured using an ellipsometer. Hydrophobic surfaces were obtained by etching the Si using 40% HF. This etching procedure removes the oxide layer (or reduces its thickness) [3]. The thickness of the oxide layer was <1 nm. A Si wafer (100) with a 30 nm thermally grown oxide layer was also examined. For stiffness imaging a well-polished epoxy-carbon fiber composite was used. The experiments are carried out using a modified Hysitron picoindenter, which sits on an AFM base and uses a Berkovich diamond tip. Detailed descriptions of the instrument and calibration procedures are given elsewhere [2]. The indenter tip shape is calibrated with a fused quartz specimen using standard procedures [4]. Contact stiffness is measured using force modulation, where a small sinusoidal AC force ranging between 20-150 nN (peak-to-peak) at 110-132 Hz is added to the applied force. The displacement amplitude and phase shift are monitored using a lock-in amplifier and used to calculate the contact stiffness. For pre-contact and apparent contact experiments the specimen approaches the indenter tip using the AFM Z piezo [2] at an approach rate of 0.5 nm/s until the phase shift reaches the preset value. Then the specimen is withdrawn at the same rate until the phase shift reaches the original value.

For indentation experiments, phase shift detection [2] is used during approach to detect the surface of the specimen before applying a load. The indentation experiments are carried out in a loading and unloading sequence. To study the effect of surface preparation all the experiments are carried out inside a dry N_2–purged glove box with humidity control. The N_2 flowed through a column of $CaSO_4$ and 5 nm molecular sieve to eliminate H_2O and organic impurities. The specimen and the instrument reached thermal equilibrium with thermal drift <0.05 nm/s before indentation tests were performed.

RESULTS AND DISCUSSION

One of the challenges in nanoindentation involves detecting the sample surface (before indentation): specimens may undergo damage on approach, and very compliant samples might not be sensed at all. Monitoring the dynamic response of the nanoindenter during tip-sample approach provides a very sensitive way to determine the location of the surface prior to indentation and provides a mode of force-distance curve acquisition [2]. We have used the above approach to examine pre-contact and apparent contact regimes on the Si surfaces. Fig. 1 shows typical force and interaction stiffness curves during approach and retraction for an as-received Si surface with the native oxide layer intact under ambient conditions (54% RH). The force curve shown here is similar to the force curve measurement in AFM. The interaction stiffness is a convolution of force gradient and contact stiffness between the tip and surface. In general it can be divided into three regimes: pre-contact, apparent- or intermittent-contact, and elastic or elasto-plastic contact regimes as shown in Fig. 1 [5]. The stiffness data initially show a downward deflection (negative with respect to the indenter spring stiffness, which has been subtracted) indicating an attractive interaction between the tip and substrate. The stiffness soon turns positive, and upon retraction shows significant hysteresis; the hysteresis is due to a real change in contact area from surface deformation and is not an experimental artifact. The corresponding force-displacement curve shows that the maximum force during indentation was 300 nN, and confirms that even at this low load that the unloading was not reversible and the deformation not elastic. The negative stiffness and adhesive force observed during retraction is

consistent with meniscus formation [6]. Estimation of surface energy from this data set and others gave results between 60 and 80 mJ/m^2, consistent with the surface energy of water (72 mJ/m^2) [7].
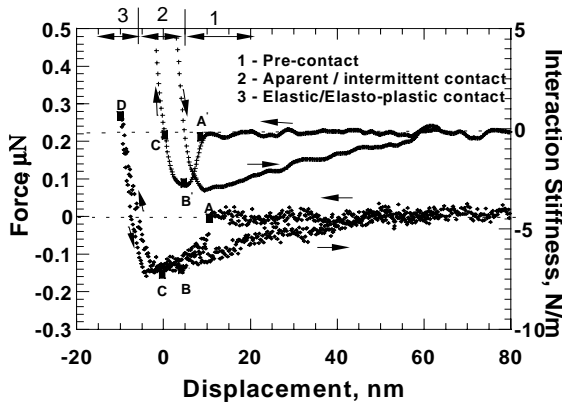

Fig. 1

Fig.1 Force (♦) and interaction stiffness (+) curves during approach (←) and retraction (→) [5].
Fig.2 The elastic loading and unloading of a hydrophilic Si surface: a) load-displacement curve and b) contact stiffness as a function of load [5].
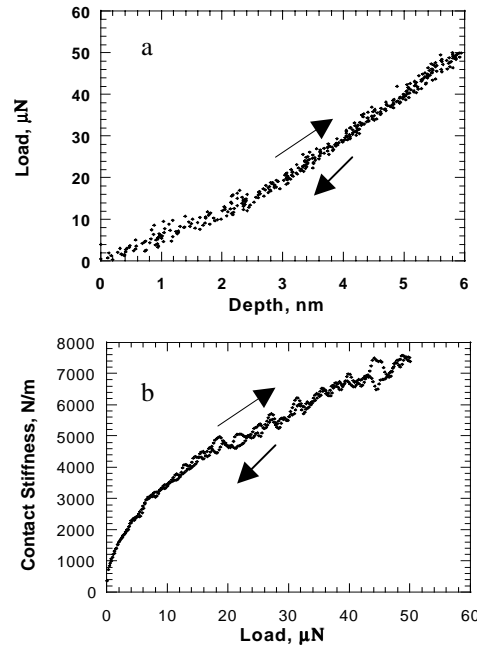

Fig. 2

Fig. 2a shows the load-displacement curve for hydrophilic Si surface at 2-5 % RH. The sample is loaded to a maximum load of 50 μN and then unloaded. The corresponding contact stiffness curve is shown in Fig. 2b. The loading and unloading is reversible and the deformation is elastic. When the load is increased to 400 μN, there is a discontinuity generally known as "pop in" in the load-displacement response (Fig. 3a). This effect has been observed in other materials [8-10]as a critical load is reached. This has been attributed to a variety of mechanisms including sudden nucleation of dislocations, micro fracture, thin film debonding or oxide layer breakthrough. Pop-in can occur due to any process which results in sudden release of strain energy.

It should be noted that Si under hydrostatic pressure undergoes a pressure-induced phase transformation from a semiconductor (cubic diamond) to metallic (β-tin) state [11,12]. When the pressure is removed, the reverse transformation occurs at distinctly lower pressures. The hardness of Si is ~11 GPa [13], which is almost equal to the pressure required for phase transformation. Several investigators have shown that the inelastic deformation in silicon during indentation is dominated by a pressure-induced phase transformation [14-16]. In Fig. 3a the pop-in occurs reproducibly in the loading curve around 220 μN. Below this critical load, however the loading and unloading curve is reversible and the deformation is totally elastic (Fig. 2a and b).

Fig. 3b shows the load-displacement curve for hydrophobic Si surfaces. The experiments were carried out at a relative humidity of 3%. It can be seen that the pop-in event still occurs but at a lower critical load (~150 μN). This could be due to the fact that HF etching does not completely remove the oxide layer. The thickness of the oxide layer apparently affects the pop-in behavior. To better understand the role of oxide thickness, several indentation experiments are carried out on 30 nm thick, thermally-grown SiO$_2$ on Si at various loads (10-1200 μN). Fig. 3c shows the load-displacement response for indentation into this oxide layer. At a load of 400 μN

the deformation is elasto-plastic and there is no evidence of pop-in. From the unloading curve the modulus and the hardness can be calculated [4] at different contact depths.
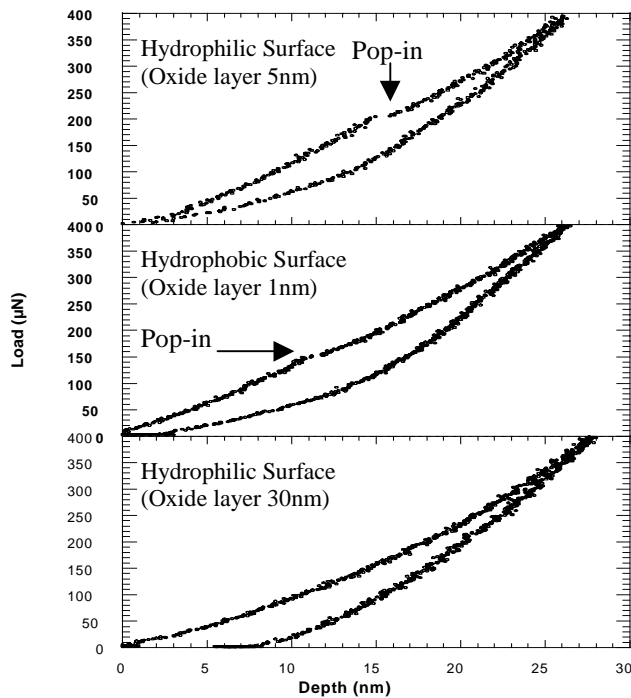

Fig. 3 The load-displacement response of Si surfaces showing pop-in and the influence of oxide layer thickness [5]
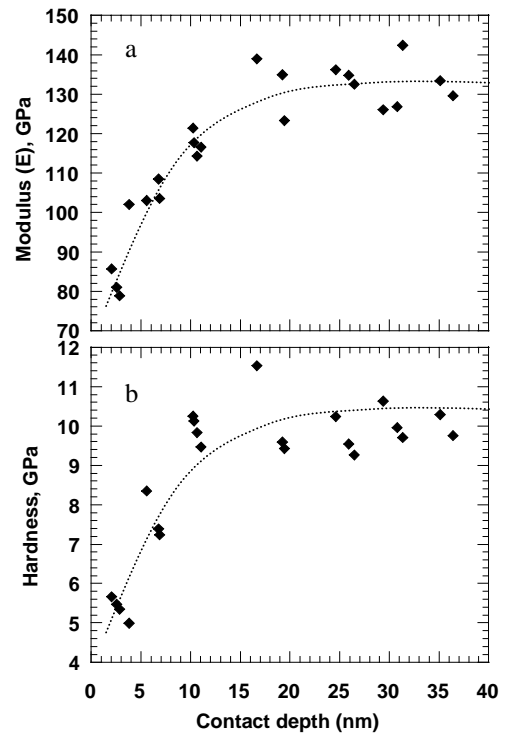
Fig. 4 Depth dependence of (a) modulus and (b) hardness of SiO_2 on Si substrate [5]

Fig. 4a shows the variation of modulus as a function of contact depth (that is the depth at which the material conforms to the shape of the indenter). At higher contact depths (>15 nm), the measured modulus is 130-140 GPa. The measured modulus compares very well with the modulus of Si (134 GPa) reported in the literature [17]. At shallow contact depths (<15 nm), the modulus decreases and approaches 70-80 GPa for depths about 1-2 nm. The modulus of fused quartz (SiO_2) is ~70 GPa. This clearly indicates that at depths ~1-2 nm the measured modulus is that of the oxide layer, (SiO_2). Also, as the depth of indentation increases, substrate influence appears since the oxide layer is more compliant than the Si substrate.

Fig. 4b shows the variation of hardness as a function of contact depth. The measured hardness has the same trend as the modulus. At shallow contact depth (1-2 nm) the hardness is ~5 GPa and it increases to 10-11 GPa at a contact depth of 12-15 nm and remains constant thereafter. As mentioned before, the hardness of Si is ~11 GPa which is almost equal to the pressure required for phase transformation. The hardness of the oxide layer is ~5 GPa (for a contact depth of 1-2 nm).

The results indicate that the critical load required for pop-in depends on the tip radius of the indenter and thickness of the oxide layer. The tip radius of the indenter used in the present experiment is ~200 nm. When the load is applied on a very thin film (~1 nm for the HF-etched surface), most of the load is supported elastically by the substrate until the mean contact pressure reaches ~11 GPa. The critical load required to reach this pressure is the pop-in load. When the mean pressure reaches 11 GPa, Si undergoes pressure-induced phase transformation and the load is no longer supported elastically by the substrate. The thin oxide film cannot accommodate the

high strain induced by the plastic deformation of the Si substrate. This results in breakthrough of the oxide layer, which appears as a pop-in in the load-displacement data. If the thickness of the oxide layer is slightly larger (5 nm for the piranha-etched surface) then the substrate is further away from the surface, the load required to reach a mean contact pressure of 11 GPa increases and the pop-in occurs at higher load. However, for a thicker oxide layer (30 nm thermally grown oxide layer) the substrate influence is significantly reduced and the plastic deformation occurs within the film itself. For a thicker oxide layer the pop-in may occur at relatively high loads but prior to pop-in the deformation is elasto-plastic. Thus the presence of an oxide layer reduces the contact pressure and increases the load required for pressure-induced phase transformation of the Si substrate.

The results presented above are all single point measurements and do not fully take advantage of the scanning capabilities provided by the AFM base. Ideally, one would like to produce an image of sample properties (e.g. map modulus and loss properties) quantitatively and quickly in an image format. Applying the force modulation technique during a scan is possible, but at low modulation frequency (due to low dynamic range, 10-300 Hz), the feedback will force the piezo to follow the indenter tip displacement, complicating the data analysis. The modulation signal that goes to the Z piezo cannot be filtered, as it will affect the feedback. To overcome this problem we have adopted an interleave-scanning technique in which in the first scan the force feedback is active and the height information is recorded. In the next adjacent scan, the feedback is shut off and only the height information from the previous scan is used to allow the Z piezo to follow the topography. The AC displacement amplitude and the phase shift during no-feedback is collected and processed to obtain contact stiffness.

Fig. 4a is the topography and 4b is the stiffness image for an epoxy-carbon fiber composite obtained using the procedure described above. The stiffness image shown here is the complex stiffness $(K + i\omega C)$, where K is the storage component of the contact stiffness, C is the damping coefficient, ω is the frequency of the force modulation (200 Hz), and $i\omega C$ is the loss component of the contact stiffness. The lighter region in the stiffness image is the epoxy and the dark round features are the carbon fibers. This stiffness image is obtained at room temperature and at a contact load of 3 µN. The quantitative stiffness image provides a first step towards quantitative mapping of modulus and loss properties of surfaces. Difficulties to overcome in converting the stiffness data to elastic modulus arise from the need to know the tip-sample penetration at each point in the image and precise knowledge of the tip shape. Despite these difficulties, such scanning techniques provide great promise towards the goal of quantitative nano mechanical properties measurements of surfaces.
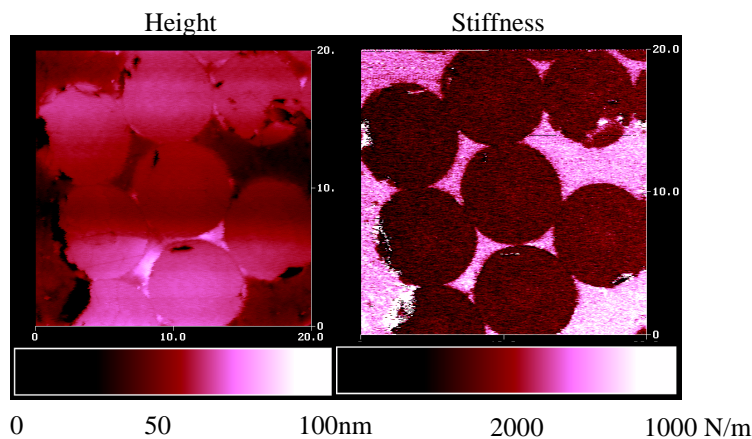

Fig. 5 An image of epoxy-carbon fiber composite (a) topography and (b) contact stiffness (complex).

CONCLUSIONS

By combining force modulation with depth sensing nanoindentation it is possible to measure the surface forces, surface energy, and interaction stiffness prior to contact. It is possible to locate the surface of the specimen without much contact damage and the mechanical response of the surface layer can be measured. The same technique can be used for stiffness imaging.

ACKNOWLEDGEMENTS

REFERENCES

1. J.B. Pethica, R. Hutchings, and W.C. Oliver, Philos. Mag. A **48**, 593 (1983).
2. S.A. Syed Asif, K.J. Wahl, and R.J. Colton, Rev. Sci. Instruments **70**, 2408 (1999).
3. M.R. Houston, R.T. Howe, and R. Maboudian, J.Appl. Phys. **81**, 3474 (1997).
4. W.C. Oliver and G.M. Pharr, J. Mater. Res. **7**,1564 (1992).
5. S.A. Syed Asif, K.J. Wahl, and R.J. Colton, J. Mater. Res., in press.
6. M. Binggeli and C.M. Mate, Appl. Phys. Lett. **65**, 415 (1994).
7. J.N. Israelachvili and D. Tabor, Proc. R. Soc. London, Ser. A **331**, 19 (1972).
8. S.A. Syed Asif and J.B. Pethica, Philos. Mag. A **76**, 1105 (1997).
9. S.G. Corcoran , R.J. Colton, E.T. Lilleodden and W.W. Gerberich, Phys. Rev. B **55**, R16057 (1997).
10. A.B. Mann and J.B. Pethica, Philos. Mag. A **79**, 577 (1999).
11. H. Minomura and H.G. Drickamer, J. Phys. Chem. Solids **23**, 451 (1962).
12. M.C. Gupta and A.L. Ruoff, J. Appl. Phys. **51**, 1072 (1980).
13. J.Z. Hu, L.D. Merkle, C.S. Menoni, and I.L. Spain, Phys. Rev. B **34**, 4679 (1986).
14. A.P. Gerk and D. Tabor, Nature **271**, 732 (1978).
15. D.R. Clarke., M.C. Kroll, P.D. Kirchner, R.F. Cook, and B.J. Hockey, Phys. Rev. Lett. **60**, 2156 (1988).
16. G.M. Pharr, W.C. Oliver and D.S. Harding, J. Mater. Res. **6**, 1129 (1991).
17. C.J. Smithells, *Smithells Metal Reference Book*, edited by E.A. Brandes (Butterworths, London, 1983), 6th edition., p. 15.